Imatinib mesylate induces mitochondria-dependent apoptosis and inhibits invasion of human pigmented villonodular synovitis fibroblast-like synovial cells

KANG CHEN[1], QIAO REN[3], XIAO-RUI HAN[2], XIAO-NAN ZHANG[2], BO WEI[2] and XI-ZHUANG BAI[2]

Departments of [1]Orthopedics and [2]Sports Medicine and Joint Surgery, The First Affiliated Hospital of China Medical University, Heping, Shenyang, Liaoning 110001; [3]Department of Medicine, Benxi Central Hospital, Benxi, Liaoning 117000, P.R. China

Received July 23, 2015; Accepted September 4, 2015

DOI: 10.3892/or.2015.4350

Abstract. Pigmented villonodular synovitis (PVNS) is a rare sarcoma-like disorder characterized by synovial lesions proliferation and invasion to articular cartilage for which no effective treatments are available. Imatinib mesylate (IM) is known to exert antitumor activity in some tumors, but its effects on PVNS fibroblast-like synoviocytes (PVNS-FLS) and the specific mechanism involved remain to be established. In the present study, the *in vitro* effects of IM on cell proliferation and survival rates were investigated in PVNS-FLS. Apoptosis induction was assessed via acridine orange/ethidium bromide (AO)/(EB) and Annexin V/PI staining as well as western blotting. The invasion ability of PVNS-FLS was evaluated by Transwell invasion chambers. IM significantly inhibited survival and invasion ability of PVNS-FLS in a dose- and time-dependent manner. The drug-treated cell groups exhibited markedly higher apoptosis, which was blocked upon pretreatment with the specific caspase-9 inhibitor Z-LEHD-FMK. Expression of cleaved caspase-9 was significantly increased and the Bcl-2 family and caspase-3 were activated following treatment with IM. Our results collectively demonstrated that IM has a strong antiproliferative effect on PVNS-FLS *in vitro*, attributable to induction of mitochondrial-dependent apoptosis in association with activation of caspase-9/-3 and the Bcl-2/Bax family, and exhibits significant inhibition on the invasion ability of PVNS-FLS, suggesting that IM may be useful as a novel treatment of this disease.

Correspondence to: Professor Xi-Zhuang Bai, Department of Sports Medicine and Joint Surgery, The First Affiliated Hospital, China Medical University, 155 Nanjing Street, Heping, Shenyang, Liaoning 110001, P.R. China
E-mail: bxzcmu@163.com

Key words: imatinib mesylate, pigmented villonodular synovitis, invasion, apoptosis, caspase

Introduction

Pigmented villonodular synovitis (PVNS); also known as tenosynovial giant cell tumor (TGCT) is a rare synovial proliferative disease with an incidence of 1.8 cases/million (1-5). Although the etiology of PVNS is unclear at present, recent evidence suggests a neoplastic nature (6-8), and malignant cases have been reported (9,10). The disease, which can involve all synovial-lined structures, particularly the knee joint, is characterized by proliferation of synovial tissues and invasion of cartilage and bone around the joints. PVNS causes clinical swelling and pain, and the diffuse form or recurrence can trigger rapid articular cartilage damage associated with severe functional impairment, eventually leading to joint replacement or even amputation (11-14). Although surgical synovectomy, either via open surgery or arthroscopy, is considered the standard treatment for PVNS (7,15), post-operative complications and limitations, including longer hospitalization and rehabilitation periods, post-operative stiffness, and in particular, high rates of recurrence are common. The post-operative recurrence rate is as high as 60% (12,16,17).

Imatinib mesylate (IM), a tyrosine kinase inhibitor, is the first-line drug of choice for chronic myeloid leukemia (18) and a gastrointestinal stromal cell tumor. A number of recent studies have reported a significant clinical effect of IM on PVNS (1,19-21). The effect of IM on PVNS was initially documented by Blay *et al* (1). In a subsequent multi-institutional retrospective study on 27 patients (74% with stable disease) by Cassier *et al* (19), treatment with IM led to symptomatic improvement in 73% patients. However, the antitumor mechanism of IM on PVNS to date is not clear. Therefore, in the present study, we examined whether IM exerts cellular antiproliferative effects and induces apoptosis in PVNS synovial cells. We further determined whether cellular apoptosis induced by IM is dependent on the mitochondrial apoptosis signaling pathways.

Materials and methods

Antibodies and reagents. IM was purchased from Selleck Chemicals (Houston, TX, USA). Z-LEHD-FMK, a caspase-9

specific inhibitor, was purchased from R&D Systems (Minneapolis, MN, USA). Dulbecco's modified Eagle's medium (DMEM) high glucose medium and fetal bovine serum (FBS) were obtained from Gibco (Gaithersburg, MD, USA). Trypsin and MTT were purchased from Sigma (St. Louis, MO, USA). Rabbit monoclonal antibody to caspase-3 and -9 were purchased from Abcam (Cambridge, UK). Rabbit polyclonal antibody to Bcl-2 and Bax were purchased from Santa Cruz Biotechnology (Santa Cruz, CA, USA).

Cell isolation and culture. PVNS fibroblast-like synoviocytes (PVNS-FLS) were isolated from synovial tissues obtained from PVNS patients at the time of knee joint synovectomy. All the patients were biopsy-proven and diagnosis was made based on conventional histological criteria. The present study was approved by the Medical Ethics Committee of the First Affiliated Hospital of China Medical University and written informed consent was obtained from all patients. FLS were purified from synovial tissue as previously published (22). Briefly, the tissue samples were minced and digested with 2 mg/ml collagenase II for 4 h and then with trypsin for 30 min at 37˚C, filtered through a 70 μm cell strainer, and cultured in DMEM containing 10% FBS, 100 U/ml penicillin and 100 mg/ml streptomycin in a humidified 5% CO_2 incubator. After overnight culture, non-adherent cells were removed by medium exchange, and adherent cells were trypsinized and passaged, and used between passages 3 and 7.

Analysis of cell proliferation and viability. The viability of PVNS-FLS cells was evaluated by the MTT [3-(4,5-dimethylthiazol-2-yl)-2,5-diphenyl-tetrazolium bromide] method. Cells/well ($8x10^3$) of FLS were incubated in a 96-well plate for 24 h, then cells were treated with different concentrations of IM with or without the caspase-9 specific inhibitor Z-LEHD-FMK, each concentration for parallel 6-wells. After incubating for another 24, 48 and 72 h, 20 μl MTT solution was added to each well. After 4 h, the medium was discarded and 150 μl DMSO was added to dissolve the formazan crystal. The absorbance was measured with a wavelength of 490 nm. Survival rate of cells (%) = experimental group A value/control group A value x 100%.

Morphology of apoptotic cells. Cells were seeded into a 6-well plate and pretreated with or without the caspase-9 inhibitor Z-LEHD-FMK at 50 μM for 2 h, then 40 μM IM was added in the test group and cultured for another 48 h. Changes in cell morphology, proliferation and ability of adherence were observed and compared under an inverted phase contrast microscope.

Apoptosis of FLS detected by Hoechst staining. FLS were seeded on aseptic cover slides into the 24-well plate and were treated with 40 μM IM in the presence or absence of Z-LEHD-FMK for 48 h. The cells were washed three times with phosphate-buffered saline (PBS) and fixed for 10 min, and then stained with Hoechst 33258 staining solution for 5 min. The staining of cell nucleus were observed under a fluorescence microscope. The apoptotic rate (%) = the number of apoptotic cells/the number of total cells x 100%.

Acridine orange/ethidium bromide (AO/EB) apoptosis assay. An AO/EB staining method was used to detect apoptosis-related morphologic changes of FLS. Cells were seeded on cover slides in a 24-well plate as described, 500 μl of freshly-prepared dual stain containing 10 mg/ml acridine orange (AO) and 10 mg/ml ethidium bromide (EB) was added to each well staining for 10 min in the dark at room temperature. The morphological changes of cell nucleus were observed under a fluorescence microscope and apoptotic rate was calculated.

Annexin V/PI apoptosis detection. After induction of apoptosis, FLS were detached by trypsinization and washed twice with cold PBS. The cells were centrifuged at 500 x g for 5 min and resuspended in 400 μl binding buffer, then 5 μl Annexin V-FITC and 10 μl propidium iodide (PI) were added and incubated in the dark at room temperature for 15 min. The samples were analyzed by a FACSCalibur (BD Biosciences) flow cytometer immediately and the data were analyzed using CellQuest software.

Cell cycle analysis. After treated with different doses of imatinib (10-40 μM) for 24 h, cells were washed twice with cold PBS and fixed in 70% ethanol for 24 h at 4˚C before analysis. Then cells were centrifuged and stained with 50 μg/ml PI and 100 μg/ml RNase A for 30 min in the dark at room temperature. The samples were analyzed by BD FACSCalibur flow cytometer and the data were analyzed using CellQuest software.

Western blot analysis. The methods for western blotting have been described (23). Briefly, the protein samples were resolved by SDS-PAGE and transferred to PVDF membranes. After transfer, the PVDF membranes were blocked with 5% (w/v) non-fat milk in TBST at room temperature for 2 h, and then incubated with the primary antibodies in the TBST buffer containing 1% (w/v) BSA at 4˚C for 16 h. Following three washes in TBST, the membranes were incubated with the appropriate secondary antibody in TBST for 2 h at room temperature. Proteins were detected by the ECL system.

Determination of the invasion ability. The invasive ability of PVNS-FLS was evaluated by the Transwell invasion system. The chamber was washed with serum-free medium, then 20 μl Matrigel was added to cover the bottom of the chamber. A Matrigel membrane was created by incubating at 37˚C for 30 min. Cells ($2x10^5$) with 200 μl serum-free DMEM medium was seeded in the upper chamber of the Transwell invasion system and 500 μl DMEM with 10% FBS was added into the lower chamber. The Transwell invasion system was incubated in a cell culture incubator for 24 h, and then the upper chamber was taken out and the cells removed from the upper surface of the membrane. Then cells invaded to the lower surface of the membrane were stained with 0.1% crystal violet and observed under an inverted phase contrast microscope. The results are presented as the mean ± SD, with three repeated experiments for each group.

Statistical analysis. Statistical analyses were performed using one-way analysis of variance (one-way ANOVA) and Bonferroni's multiple comparisons post tests were used as needed. Data are presented as the mean ± SD from a minimum of three independent experiments performed in

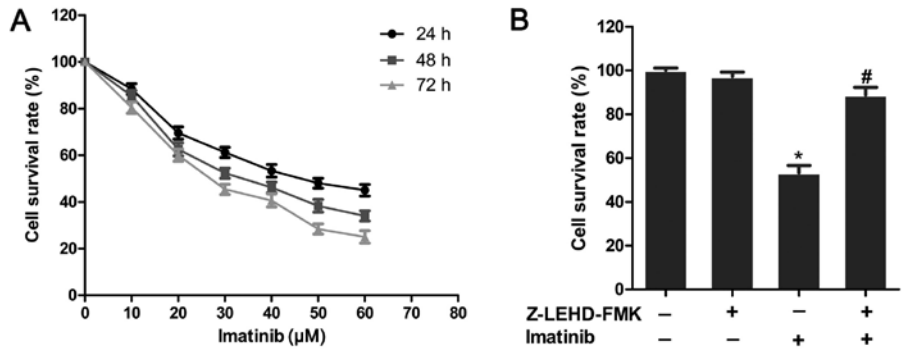

Figure 1. Inhibitory effect of IM on PVNS-FLS measured using MTT. (A) Cells were incubated with increasing concentrations of IM (10-60 μM) for 24, 48 and 72 h. (B) Cells were treated with the caspase-9 inhibitor, Z-LEHD-FMK (50 μM), with or without IM (40 μM) for 48 h (*P<0.05 vs. the control group, $^{\#}$P<0.05 vs. IM alone group).

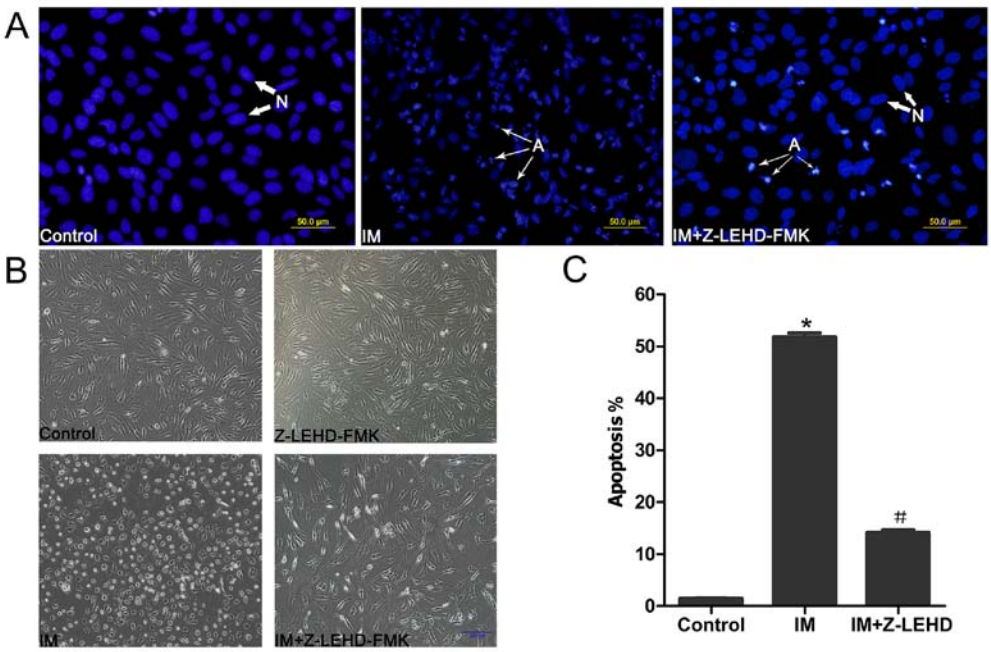

Figure 2. Morphological changes of apoptotic cells treated with different drugs. (A) PVNS-FLS were treated with IM (40 μM) alone or in combination with Z-LEHD-FMK (50 μM) for 48 h, and cell nuclei stained with Hoechst 33258 and observed under a fluorescence microscope at a magnification of x400 (N, normal nuclei; A, apoptotic nuclei.) (B) Cells were treated with different drugs and morphological features observed under an inverted phase-contrast microscope at a magnification of x100. (C) Ratio of apoptotic cells stained with Hoechst 33258. Cells with condensed or fragmented nuclei were considered apoptotic. The number of apoptotic cells was counted in five random fields/well. Experiments were repeated three times. (*P<0.01 vs. the control group, $^{\#}$P<0.01 vs. the IM alone group).

triplicate. P<0.05 was considered to indicate a statistically significant result.

Results

IM reduces the viability of PVNS-FLS. To determine the effects of IM on proliferation of PVNS-FLS, the MTT assay was carried out with different concentrations of IM (10-60 μM) for 24, 48 and 72 h. As shown in Fig. 1A, IM significantly inhibited the survival of PVNS-FLS cells in a dose- and time-dependent manner. The IC_{50} value for 48 h was ~40 μM, which was taken as the effective drug concentration in subsequent experiments. Upon pre-treatment of cells with the caspase-9-specific inhibitor Z-LEHD-FMK (50 μM), the antiproliferative effect was blocked (P<0.05), and survival rates were markedly enhanced (Fig. 1B). We observed no differences in survival rates (P>0.05), compared with the control group, upon the addition of Z-LEHD-FMK alone, suggesting a critical role of caspase-9 in IM-induced apoptosis of PVNS-FLS.

Morphological changes of apoptotic cells. Morphological changes in FLS after apoptosis induction with IM were examined under an inverted phase-contrast microscope. Cells in the control and Z-LEHD-FMK groups presented a slender fiber-like appearance and attached uniformly to the dish. In contrast, in the drug-treated groups, the cell shape became small and round, with some cells being non-adherent and suspended in medium (Fig. 2B). To further resolve the morphology of apoptotic nuclei, Hoechst 33258 staining was

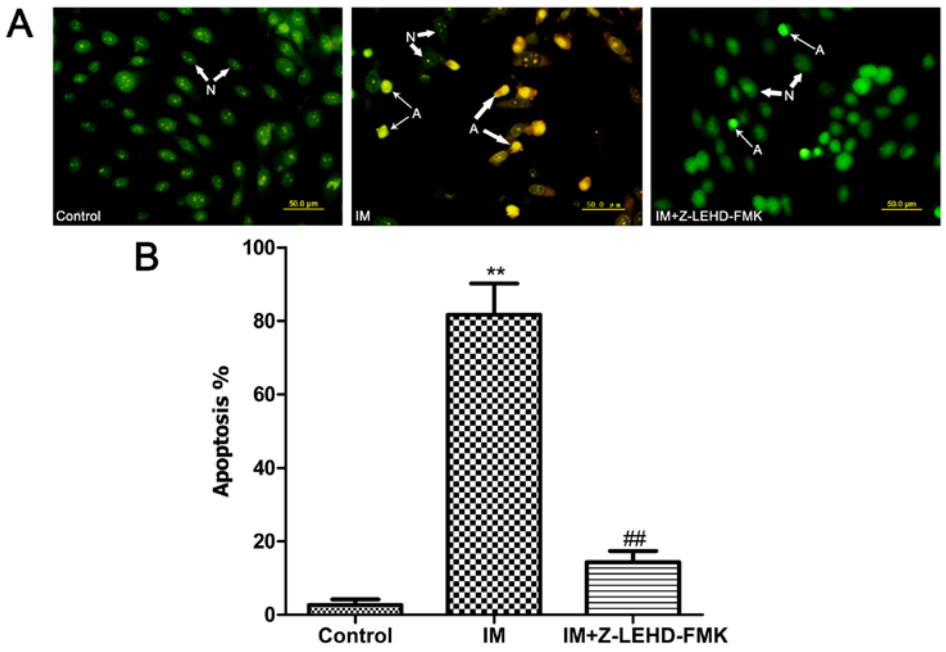

Figure 3. Apoptotic changes of cell nuclei induced by IM in PVNS-FLS. (A) Cells were treated withIM (40 μM) alone or in combination with Z-LEHD-FMK (50 μM) for 48 h and cell nuclei were stained with acridine orange/ethidium bromide (AO/EB) staining and observed under a fluorescence microscope. Cells with condensed or fragmented nuclei were considered apoptotic and early apoptotic nuclei presented as green or light yellow, late apoptotic nuclei presented as orange or red. (N, normal nuclei; A, apoptotic nuclei; thick arrow, late apoptosis; thin arrow, early apoptosis). (B) Quantitative assessment of apoptosis rate. Experiments were repeated three times. (**P<0.01 vs. the control group, $^{\#\#}$P<0.01 vs. the IM alone group).

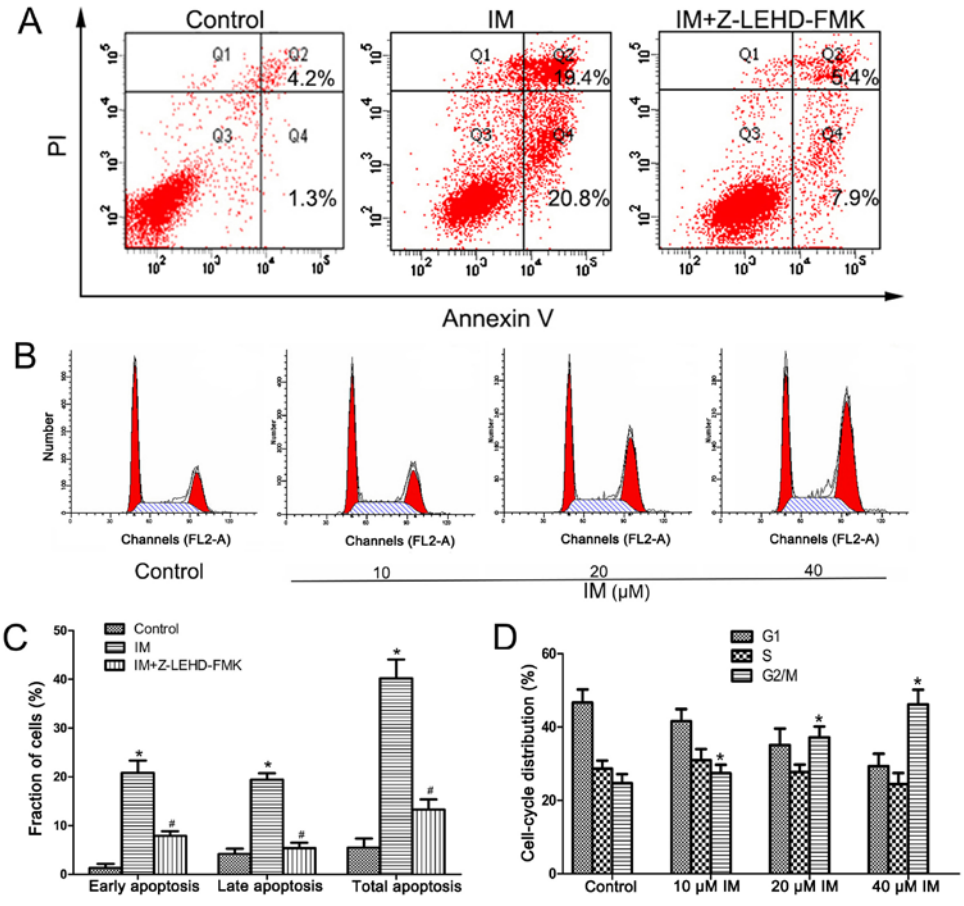

Figure 4. Determination of apoptosis in PVNS-FLS via Annexin V/PI staining and cell cycle arrest with flow cytometry. (A) Cells were stained with FITC-conjugated Annexin V and PI after induction of apoptosis, and monitored using flow cytometry. (B) FLS treated with imatinib mesylate for 48 h or left untreated were subjected to propidium iodide (PI) staining and flow cytometry. (C) Histogram analysis of apoptotic ratio. Early apoptosis is localized in the bottom right area and late apoptosis in the top right area (*P<0.05 vs. the control group, $^{\#}$P<0.05 vs. the IM group). (D) Cell cycle distribution of IM-treated cells revealed G2/M phase arrest (*P<0.05 vs. the control group). Experiments were repeated three times and results are expressed as mean ± SD.

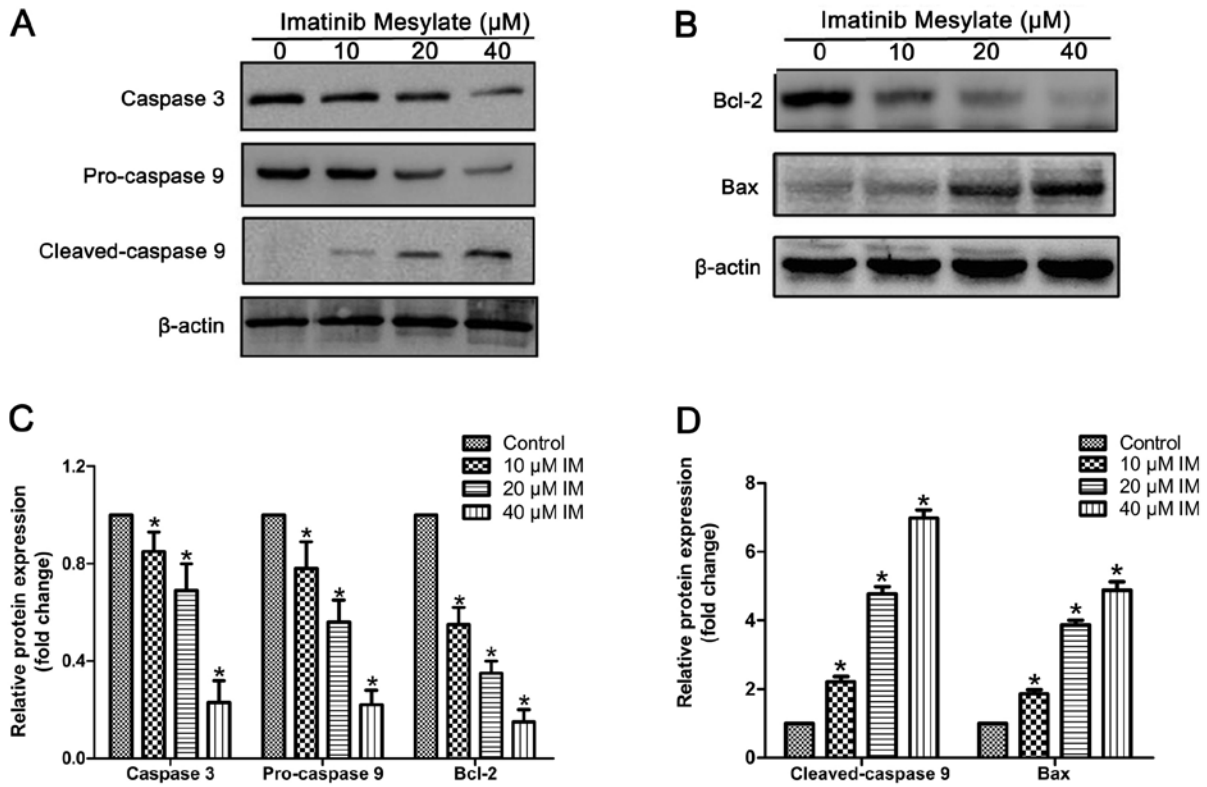

Figure 5. Western blot analysis of apoptosis-related proteins. (A) Effects of IM on protein expression of pro- and cleaved caspase-9 and -3 in PVNS-FLS after treatment of cells for 48 h. (B) Effects of IM on protein expression of Bcl-2 and Bax in PVNS-FLS after treatment of cells for 48 h. (C and D) Quantitative analysis of relative protein expression using a histogram. Data are expressed as means ± SD. All experiments were repeated three times (*P<0.05 vs. the control group).

performed. FLS in the control group showed regular round and normal nuclei with almost no sign of apoptosis. In contrast, cells treated with IM exhibited condensed, fragmented and crescent-shaped nuclei characteristic of apoptosis (Fig. 2A). Apoptosis was blocked upon pretreatment with the caspase-9 inhibitor Z-LEHD-FMK (50 μM). The percentage of apoptosis index was significantly different between groups. The control group contained a limited percentage of apoptotic cells (1.45±0.097%), which was markedly increased in the drug-treated group (51.74±1.75%). After the addition of Z-LEHD-FMK, the apoptotic rate was markedly decreased in the IM-treated group (14.14±1.07%; Fig. 2C).

Apoptotic changes of cell nuclei stained with AO/EB staining. In order to observe the changes in nuclear morphology of apoptosis more clearly, an AO/EB double staining method was used. As shown in Fig. 3, after treated with IM, the number of apoptotic cells was increased greatly, and this trend is blocked with the addition of Z-LEHD-FMK, which is consistent with the previous results.

IM induces caspase-9-dependent apoptosis in PVNS-FLS. The Annexin V/PI staining assay was employed to further confirm the apoptotic effect of imatinib. As shown in Fig. 4A, the apoptosis ratio of the IM-treated group was significantly higher than that of the control group (P<0.01). The apoptotic cell population was significantly reduced in the presence of Z-LEHD-FMK (from 41.52±3.87 to 14.25±2.08%) (Fig. 4C), clearly indicating that apoptosis is induced by IM via a caspase-9-dependent pathway.

IM induces G2/M arrest in PVNS-FLS. PI staining data revealed that IM causes cell cycle arrest at the G2/M phase in PVNS-FLS. Upon exposure of cells to different concentrations of drugs as above, the cell number at the G2/M phase was substantially increased from 24.68±2.53 to 46.17±4.62% in the 40 μM IM-treated group while the number of cells at the G1 phase decreased from 46.66±3.66 to 29.35±3.40% (Fig. 4D).

IM activates caspase-9/-3 and the Bcl-2 family in PVNS-FLS. To further clarify the specific signaling pathways involved in the apoptotic effects of IM, we evaluated the appropriate protein expression patterns using western blotting. As shown in Fig. 5, expression of cleaved caspase-9 (35 kDa) was markedly increased upon IM treatment in a dose-dependent manner. Conversely, we observed a significant decrease in pro-caspase-9 and pro-caspase-3 levels, indicating activation of caspase-9 and -3. The key members of the Bcl-2 family, Bcl-2 and Bax, were analyzed to determine the effects of IM on expression patterns of upstream apoptotic proteins. Expression of Bax was considerably increased while that of Bcl-2 was decreased by IM in a dose-dependent manner.

IM inhibits the invasion ability of PVNS-FLS. A Transwell invasion assay was used to evaluate the invasion ability of

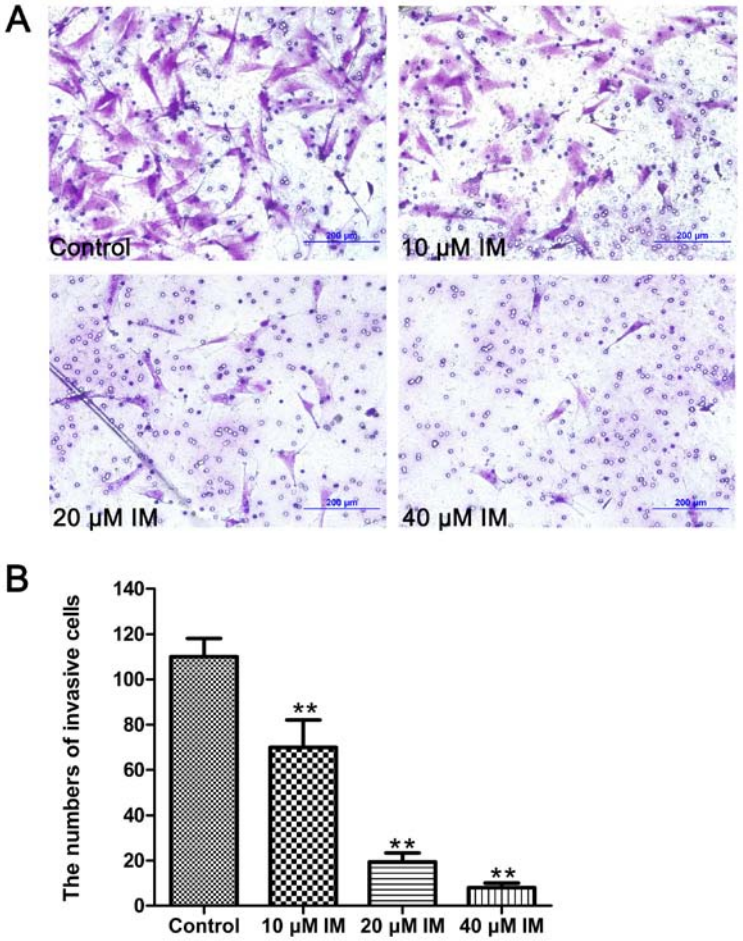

Figure 6. The invasive ability of PVNS-FLS after treated with different drugs. (A) After incubated for 24 h, cells that passed through the polycarbonate membrane were stained with crystal violet and observed under an inverted phase contrast microscope. (B) Histogram analysis of cells passed through Transwell invasion chambers. (**P<0.01 vs. the control group).

PVNS-FLS after treated with different drugs. As shown in Fig. 6, cells in the drug groups that crossed through the polycarbonate membrane of the Transwell invasion chamber were significantly less than that in the control group (P<0.01), and showed a dose-dependent manner. These data indicated that IM had a strong inhibitory effect on the invasion ability of PVNS-FLS.

Discussion

Pigmented villonodular synovitis (PVNS) is a rare synovial proliferative disorder, which is almost always monoarticular, and in 80% of cases, affects the knee joint. The disorder can present either as a localized (LPVNS) or diffuse form (DPVNS), the latter being more common (5,24-27). Although its etiology is unclear, recent studies have suggested a type of sarcoma. The disease, particularly the diffuse form, displays several tumor characteristics. PVNS presents as an aggressive tumor that invades adjacent articular cartilage and extra-articular tissues and causes rapid, irreversible joint impairment. Unfortunately, it is almost impossible to excise the extensive mass in its entirety via synovectomy without causing joint damage, since almost no boundaries exist between the lesions and normal tissues. Hence, there remains an urgent unmet medical need for safe and effective treatments for this disease.

Imatinib mesylate (IM) is a known antitumor agent for chronic myloid leukemia (CML) (28) and gastrointestinal stromal tumors (GIST) (29). Recent research has revealed a critical role in controlling tumor growth and relieving clinical symptoms of patients with PVNS, supporting its utility as a novel therapeutic agent for the disease (1,19-21). Blay *et al* (1) reported the effect of IM on a PVNS patient with a relapse of PVNS of the right elbow for the first time. Complete remission was observed after treatment with imatinib at a dose of 400 mg/day for 5 months. Subsequent studies by Ravi *et al* (20) and Cassier *et al* (19) further confirmed the therapeutic effect of imatinib on PVNS in clinic. However, the antitumor mechanism is unknown and related basic research is lacking.

In the present study, we treated PVNS synovial cells with different concentrations of IM for specific periods of time. Survival rates showed a clear dose- and time-dependent trend. After 48 h of treatment, the survival rate of cells was reduced from 85.42±2.37 to 34.0±2.58% with increasing concentrations of IM from 10 to 60 μM. The survival rate declined from 53.37±3.86 to 40.68±2.59% with extended incubation times at a drug concentration of 40 μM (Fig. 1A). Previous studies have speculated that the caspase-9-based mitochondrial apoptotic pathway may play a key role in the cell killing effect of imatinib in CML (30). To ascertain whether the mechanism underlying the antiproliferative effects of IM

in PVNS-FLS involves activation of caspase-9, cells were treated with Z-LEHD-FMK, a specific caspase-9 inhibitor. Upon treatment with Z-LEHD-FMK alone, no differences in cell viability were evident, compared with the control group, suggesting no effect of the inhibitor on proliferation. However, treatment with Z-LEHD-FMK in combination with IM led to a significant improvement in cell survival rates (Fig. 1B), indicating a central role of caspase-9 in IM-induced apoptosis. Significant changes were observed in the general morphology of cells treated with IM, including loss of normal shape and adhesion ability (Fig. 2B). The results collectively suggest that IM has an obvious killing effect on PVNS-FLS and effectively reduces cell viability *in vitro*. Hoechst and AO/EB staining data further supported the apoptotic effect of IM. Characteristic morphological changes of apoptosis appeared gradually with the addition of IM. Nuclei became condensed and crescent shaped with subsequent chromatin dissolution, breakdown, and fragmentation, indicative of the late stages of apoptosis (Figs. 2A and 3).

The Annexin V/PI staining assay additionally validated the apoptosis-inducing effect of IM. Upon IM treatment, we observed a significant increase in apoptosis rates, both early and late-stage, compared with the control group (Fig. 4A and C). Consistent with previous results, apoptosis was blocked upon the addition of Z-LEHD-FMK. PI staining data revealed that IM causes cell cycle arrest in FLS. Treated cells displayed apparent G2/M phase arrest with increasing drug concentrations (Fig. 4B and D). Our findings suggest that when cells are treated with IM, mitosis is blocked, which affects the proliferation and viability of PVNS-FLS. With increasing drug concentrations, the killing effect is fulfilled through induction of apoptosis. Pretreatment of cells with the caspase-9 inhibitor Z-LEHD-FMK, blocked apoptosis, implying that IM-induced cell death occurs via a caspase-9-dependent pathway.

Caspase-9, an essential initiator caspase, is a primary caspase of the mitochondrial apoptosis pathway. The mitochondrial pathway is initiated within cells, and the mitochondrion is a key location (31). Following exposure to various apoptotic stimuli in mitochondria, Bcl-2 family members are activated, including the anti-apoptotic protein, Bcl-2 and the pro-apoptotic protein, Bax. Consequently, the Bax/Bcl-2 ratio is increased, which enhances the permeability of the mitochondrial outer membrane. As a result, a type of soluble mitochondrial intramembrane protein (SIMP), cytochrome *c* (cyt *c*), is released into the cytoplasm that binds the apoptosis protease-activating factor-1 (Apaf-1). Subsequently, pro-caspase-9 interacts with the caspase recruitment domain (CARD) of Apaf-1, forming the apoptosome whereby caspase-9 is activated and stimulates the caspase-3 effector, in turn, driving the terminal events of apoptosis (31-34).

To elucidate the mechanism underlying apoptosis induction by IM in PVNS-FLS, we employed western blot analysis in the current investigation. IM-treated PVNS-FLS showed significant activation of caspase-9 and -3 in a dose-dependent manner. The level of cleaved caspase-9 (35 kDa) was greatly increased, and conversely, pro-caspase-9 and pro-caspase-3 levels were significantly decreased. Expression of pro-apoptotic Bax was significantly increased while that of anti-apoptotic Bcl-2 was reduced, indicating activation of the Bcl-2 family members as described above. Our findings collectively suggest that caspase-related apoptosis plays a critical role in the IM-induced cell killing effect, particularly the mitochondrial pathway where caspase-9 is a central player. The inhibitory effects of Z-LEHD-FMK on apoptosis further confirmed this theory.

In addition, invasion to tissues around joints is the main feature of PVNS. Synovial lesions invade the ligaments, bone and cartilage around the joints, leading to rapid degeneration and functional impairment of the joints. In addition, this is also the main reason why surgical synovectomy can not excise the extensive lesions and eventually cause a high rate of recurrence. Thus, a treatment to inhibit the synovial lesions invasion is urgently needed. In the present study, we found that IM exhibited significant inhibition on the invasion ability of PVNS-FLS *in vitro* detected by a Transwell invasion assay (Fig. 6), which makes it a potential treatment of the disease.

Strong erosion of adjacent tissue and higher recurrence rate has been a critical dilemma for surgeons dealing with PVNS in the clinic. Traditional surgical and radiation therapy procedures are not effective and increase the suffering of patients. Several chemotherapy drugs have been shown to prevent cell proliferation or kill tumor cells by inducing apoptosis in the clinic. It remains to be established whether IM has a similar effect on PVNS. In our experiments, IM exerted significant inhibitory activity on the viability and proliferation of PVNS-FLS *in vitro*, and apoptotic effects were evident from the morphological changes of cells under the fluorescence microscope and results of Annexin V/PI staining. Accordingly, we concluded that the cell killing effect of IM is attributable to induction of apoptosis. To further establish the specific signaling pathways underlying IM-induced apoptosis, cells were treated with the caspase-9 specific inhibitor Z-LEHD-FMK. IM-induced apoptosis was significantly blocked upon co-treatment with Z-LEHD-FMK, implying a key role of caspase-9. Expression of cleaved caspase-9 was significantly enhanced and the Bcl-2 family and caspase-3 activated following treatment of PVNS-FLS with IM. Furthermore, IM also exerted significant inhibition on the invasion ability of PVNS-FLS.

In summary, IM exerts a significant antiproliferative effect on PVNS-FLS *in vitro* through induction of apoptosis dependent on mitochondrial apoptosis pathway by the activation of caspase-9/-3 and the Bcl-2 family. The present study is the first to report the induction of apoptosis of IM on PVNS-FLS, which provides theoretical bases for clinical treatment of patients with PVNS. We also observed that IM greatly inhibits the invasion ability of PVNS-FLS, which may eventually inhibit the erosion to tissue around joints in clinical. However, further studies, including *in vivo* trials, are required to confirm the current findings and elucidate the precise mechanisms underlying IM-induced apoptosis. We believe that extended biomedicine and biotechnology analyses will facilitate the development of a novel, clinically applicable IM-based therapy for PVNS.

Acknowledgements

This study was supported by the National Natural Science Foundation of China (81071449).

References

1. Blay JY, El Sayadi H, Thiesse P, Garret J and Ray-Coquard I: Complete response to imatinib in relapsing pigmented villonodular synovitis/tenosynovial giant cell tumor (PVNS/TGCT). Ann Oncol 19: 821-822, 2008.
2. Gu HF, Zhang SJ, Zhao C, Chen Y and Bi Q: A comparison of open and arthroscopic surgery for treatment of diffuse pigmented villonodular synovitis of the knee. Knee Surg Sports Traumatol Arthrosc 22: 2830-2836, 2014.
3. Ottaviani S, Ayral X, Dougados M and Gossec L: Pigmented villonodular synovitis: A retrospective single-center study of 122 cases and review of the literature. Semin Arthritis Rheum 40: 539-546, 2011.
4. Lavrador JP, Oliveira E, Gil N, Francisco AF and Livraghi S: C1-C2 pigmented villonodular synovitis and clear cell carcinoma: Unexpected presentation of a rare disease and a review of the literature. Eur Spine J 24 (Suppl 4): S465-S471, 2015.
5. Myers BW, Masi AT and Feigenbaum SL: Pigmented villonodular synovitis and tenosynovitis: A clinical epidemiologic study of 166 cases and literature review. Medicine 59: 223-238, 1980.
6. West RB, Rubin BP, Miller MA, Subramanian S, Kaygusuz G, Montgomery K, Zhu S, Marinelli RJ, De Luca A, Downs-Kelly E, *et al*: A landscape effect in tenosynovial giant-cell tumor from activation of CSF1 expression by a translocation in a minority of tumor cells. Proc Natl Acad Sci USA 103: 690-695, 2006.
7. Nassar WA, Bassiony AA and Elghazaly HA: Treatment of diffuse pigmented villonodular synovitis of the knee with combined surgical and radiosynovectomy. HSS J 5: 19-23, 2009.
8. Fiocco U, Sfriso P, Lunardi F, Pagnin E, Oliviero F, Scagliori E, Cozzi L, Vezzù M, Molena B, Scanu A, *et al*: Molecular pathways involved in synovial cell inflammation and tumoral proliferation in diffuse pigmented villonodular synovitis. Autoimmun Rev 9: 780-784, 2010.
9. Bertoni F, Unni KK, Beabout JW and Sim FH: Malignant giant cell tumor of the tendon sheaths and joints (malignant pigmented villonodular synovitis). Am J Surg Pathol 21: 153-163, 1997.
10. Imakiire N, Fujino T, Morii T, Honya K, Mochizuki K, Satomi K and Fujioka Y: Malignant pigmented villonodular synovitis in the knee - report of a case with rapid clinical progression. Open Orthop J 5: 13-16, 2011.
11. Kaneko K, Nakahara D, Tobe M, Iwase H, Inoue Y, Ohbayashi O and Kurosawa H: Pigmented villonodular synovitis of the ankle in an adolescent. Int Orthop 24: 234-237, 2000.
12. Park G, Kim YS, Kim JH, Lee SW, Song SY, Choi EK, Yi SY and Ahn SD: Low-dose external beam radiotherapy as a postoperative treatment for patients with diffuse pigmented villonodular synovitis of the knee: 4 recurrences in 23 patients followed for mean 9 years. Acta Orthop 83: 256-260, 2012.
13. Snoots WM, Watkins D, Dockery D, Mennel R and Cheek BS: Pigmented villonodular synovitis responsive to imatinib therapy. Proc 24: 134-138, 2011.
14. Ray RA, Morton CC, Lipinski KK, Corson JM and Fletcher JA: Cytogenetic evidence of clonality in a case of pigmented villonodular synovitis. Cancer 67: 121-125, 1991.
15. Chen WM, Wu PK and Liu CL: Simultaneous anterior and posterior synovectomies for treating diffuse pigmented villonodular synovitis. Clin Orthop Relat Res 470: 1755-1762, 2012.
16. Nakahara H, Matsuda S, Harimaya K, Sakamoto A, Matsumoto Y, Okazaki K, Tashiro Y and Iwamoto Y: Clinical results of open synovectomy for treatment of diffuse pigmented villonodular synovitis of the knee: Case series and review of literature. Knee 19: 684-687, 2012.
17. Nishida Y, Tsukushi S, Nakashima H, Sugiura H, Yamada Y, Urakawa H, Arai E and Ishiguro N: Osteochondral destruction in pigmented villonodular synovitis during the clinical course. J Rheumatol 39: 345-351, 2012.
18. Liu XY, Yang YF, Wu CT, Xiao FJ, Zhang QW, Ma XN, Li QF, Yan J, Wang H and Wang LS: Spred2 is involved in imatinib-induced cytotoxicity in chronic myeloid leukemia cells. Biochem Biophys Res Commun 393: 637-642, 2010.
19. Cassier PA, Gelderblom H, Stacchiotti S, Thomas D, Maki RG, Kroep JR, van der Graaf WT, Italiano A, Seddon B, Dômont J, *et al*: Efficacy of imatinib mesylate for the treatment of locally advanced and/or metastatic tenosynovial giant cell tumor/pigmented villonodular synovitis. Cancer 118: 1649-1655, 2012.
20. Ravi V, Wang WL and Lewis VO: Treatment of tenosynovial giant cell tumor and pigmented villonodular synovitis. Curr Opin Oncol 23: 361-366, 2011.
21. Stacchiotti S, Crippa F, Messina A, Pilotti S, Gronchi A, Blay JY and Casali PG: Response to imatinib in villonodular pigmented synovitis (PVNS) resistant to nilotinib. Clin Sarcoma Res 3: 8, 2013.
22. Zimmermann T, Kunisch E, Pfeiffer R, Hirth A, Stahl HD, Sack U, Laube A, Liesaus E, Roth A, Palombo-Kinne E, *et al*: Isolation and characterization of rheumatoid arthritis synovial fibroblasts from primary culture - primary culture cells markedly differ from fourth-passage cells. Arthritis Res 3: 72-76, 2001.
23. Wessel D and Flügge UI: A method for the quantitative recovery of protein in dilute solution in the presence of detergents and lipids. Anal Biochem 138: 141-143, 1984.
24. Granowitz SP, D'Antonio J and Mankin HL: The pathogenesis and long-term end results of pigmented villonodular synovitis. Clin Orthop Relat Res 114: 335-351, 1976.
25. Schwartz HS, Unni KK and Pritchard DJ: Pigmented villonodular synovitis. A retrospective review of affected large joints. Clin Orthop Relat Res 247: 243-255, 1989.
26. Tyler WK, Vidal AF, Williams RJ and Healey JH: Pigmented villonodular synovitis. J Am Acad Orthop Surg 14: 376-385, 2006.
27. Dines JS, DeBerardino TM, Wells JL, Dodson CC, Shindle M, DiCarlo EF and Warren RF: Long-term follow-up of surgically treated localized pigmented villonodular synovitis of the knee. Arthroscopy 23: 930-937, 2007.
28. Guilhot F: Indications for imatinib mesylate therapy and clinical management. Oncologist 9: 271-281, 2004.
29. Sawyers CL: Imatinib GIST keeps finding new indications: Successful treatment of dermatofibrosarcoma protuberans by targeted inhibition of the platelet-derived growth factor receptor. J Clin Oncol 20: 3568-3569, 2002.
30. Du Y, Wang K, Fang H, Li J, Xiao D, Zheng P, Chen Y, Fan H, Pan X, Zhao C, *et al*: Coordination of intrinsic, extrinsic, and endoplasmic reticulum-mediated apoptosis by imatinib mesylate combined with arsenic trioxide in chronic myeloid leukemia. Blood 107: 1582-1590, 2006.
31. Hu Q, Wu D, Chen W, Yan Z, Yan C, He T, Liang Q and Shi Y: Molecular determinants of caspase-9 activation by the Apaf-1 apoptosome. Proc Natl Acad Sci USA 111: 16254-16261, 2014.
32. Jin Z and El-Deiry WS: Overview of cell death signaling pathways. Cancer Biol Ther 4: 139-163, 2005.
33. Luo X, Budihardjo I, Zou H, Slaughter C and Wang X: Bid, a Bcl2 interacting protein, mediates cytochrome *c* release from mitochondria in response to activation of cell surface death receptors. Cell 94: 481-490, 1998.
34. Mutlu A, Gyulkhandanyan AV, Freedman J and Leytin V: Activation of caspases-9, -3 and -8 in human platelets triggered by BH3-only mimetic ABT-737 and calcium ionophore A23187: Caspase-8 is activated via bypass of the death receptors. Br J Haematol 159: 565-571, 2012.